International Journal of Fracture **130:** 765–785, 2004.

Mode III crack growth in linear hardening materials with strain gradient effects

ENRICO RADI[1,*] and MASSIMILIANO GEI[2]
[1] *Dipartimento di Scienze e Metodi dell'Ingegneria, Università di Modena e Reggio Emilia, Viale Allegri, 13 – I-42100 Reggio Emilia, Italia*
[2] *Dipartimento di Ingegneria Meccanica e Strutturale, Università di Trento, Via Mesiano, 77 – I-38050 Trento, Italia*
[*] *Author for correspondence (E-mails: eradi@unimore.it (Radi); mgei@ing.unitn.it (Gei))*

Received 29 September 2002; accepted in revised form 23 August 2004

Abstract. The flow-theory version of couple stress strain gradient plasticity is adopted for investigating the asymptotic fields near a steadily propagating crack-tip, under Mode III loading conditions. By incorporating a material characteristic length, typically of the order of few microns for ductile metals, the adopted constitutive model accounts for the microstructure of the material and can capture the strong size effects arising at small scales. The effects of microstructure result in a substantial increase in the singularities of the skew-symmetric stress and couple stress fields, which occurs also for a small hardening coefficient. The symmetric stress field turns out to be non-singular according to the asymptotic solution for the stationary crack problem in linear elastic couple stress materials. The performed asymptotic analysis can provide useful predictions about the increase of the traction level ahead of the crack-tip due to the sole contribution of the rotation gradient, which has been found relevant and non-negligible at the micron scale.

Key words: Crack-tip plasticity, crack propagation, strain gradient effects, elastic–plastic material, asymptotic analysis.

1. Introduction

Ductile materials exhibit size effect when subject to inhomogeneous plastic deformation at the micron scale. This phenomenon has been discovered and established in a large number of experimental investigations, that range from wire torsion to bending of thin films to microindentation, performed on samples having the characteristic size of the order of few microns (cf. Hutchinson, 2000), and is intimately connected to the accumulation of geometrically necessary dislocations, which are responsible for the strain gradient effects (see Gao and Huang, 2003). As noted by Hutchinson (2000), classical plasticity theories fail in characterizing the constitutive behaviour of ductile materials at the micron scale as well as in predicting the size effect, due to the lack of a length scale. Enhanced constitutive models are therefore required, which account for the microstructure of the material and the presence of dislocations by incorporating one or more characteristic lengths. For this purpose, several strain gradient plasticity models based on phenomenological theories have been proposed, e.g., by Acharya and Bassani (2000), Aifantis (1984), Chen and Wang (2002), Fleck and Hutchinson (1993, 1997, 2001). While in the Acharya–Bassani formulation, strain gradients are assumed only as internal variables which affect the values of

the tangent moduli in a standard J_2-flow theory, the other models introduce higher-order stresses and non-standard boundary conditions. In particular, in a first attempt, Fleck and Hutchinson (1993) presented the couple stress (CS) theory of strain gradient plasticity which involves strain rotation gradients, and, thus, only an intrinsic material length ℓ was introduced, a way also pursued by Chen and Wang (2002). While such approaches proved to be quite accurate in the prediction of wire torsion and bending of thin films, with ℓ of the order of few microns for metals, they failed to estimate results of micro-indentation tests and void growth where also stretch gradients come into play. Therefore, a strain gradient theory (Fleck and Hutchinson, 1997), which assumes displacements and plastic strains as primary variables, was proposed and recently reformulated (Fleck and Hutchinson, 2001) by the same authors, in order to incorporate up to three material length scales. Alternatively, by starting from a micromechanics approach based on Taylor's dislocation model for plastic work hardening, Gao et al. (1999) developed the mechanism-based strain gradient (MSG) plasticity theory, which provides a link between the mesoscale strain gradient plasticity level and the microscale dislocation mechanics.

Incorporation of strain gradients in the constitutive description of ductile materials may improve considerably the estimation of the stress traction level ahead of the crack-tip required for the occurrence of cleavage or atomic decohesion during the crack growth process, experimentally observed in ductile metals by Elssner et al. (1994). Several analyses have been carried out to investigate the effects of the aforementioned constitutive models in fracture mechanics. Xia and Hutchinson (1996) and Huang et al. (1997, 1999) examined mode I and mode II asymptotic and full-field solutions for a stationary crack with the CS theory. They found that the stress field dominates the couple stress field and then the traction level ahead of the crack-tip does not increase substantially. For the corresponding mode I crack propagation problem, Radi (2003) found that the CS field is dominant near to the crack-tip and produces a remarkable increase of the stress singularity, even for low hardening. In a numerical simulation, Wei and Hutchinson (1997) analysed the effects of stretch gradients (SG plasticity) in steady-state crack growth and found a sensible amplification of the traction level ahead of the crack-tip. However, the analyses of Chen et al. (1999) for a stationary crack-tip show that an extremely small zone ahead of the crack-tip (less than 0.1 μm) is characterised by a compressive stress traction for mode I loading conditions, which results in a physically unacceptable situation and rises some concerns about the application of SG plasticity to fracture mechanics problems. Crack mechanics investigation based on MSG plasticity have been performed by Shi et al. (2000) and Jiang et al. (2001). In the former paper it has been established that the crack-tip field in MSG is not separable at very small distance from the crack-tip, so that only numerical or analytical full-field investigations can be performed. In the latter, an increase in the effective stress and in the stress singularity is observed for a stationary crack with respect to the classical HRR field at a distance from the crack-tip almost lower than $\ell/3$, where ℓ is a length scale similar to that of the CS theory.

The problem of mode III crack propagation within the classical J_2-flow theory was first analysed by Amazigo and Hutchinson (1977) and Ponte Castañeda (1987) for materials which display linear and isotropic hardening and extended by Bigoni and Radi (1996) to mixed isotropic/kinematic hardening. These investigations found that the strength of the stress singularity turns out to be extremely weak for the

typically small values of the strain hardening for ductile metals. The effects of elastic strain gradients on the stress concentration at the tip of a mode III stationary crack were considered by Vardoulakis et al. (1996), Zhang et al. (1998), Fannjiang et al. (2002) and Georgiadis (2003). While in Vardoulakis et al. (1996) and Fannjiang et al. (2002), strain gradients are introduced through the second gradient of displacement, in Zhang et al. (1998) rotation gradients are considered, then adopting a couple stress theory which is the specialisation of the model adopted here when plasticity is absent. The results of Zhang et al. (1998) indicate that the effects of rotation gradients increase the stress singularity at the crack-tip from $r^{-1/2}$, as obtained for classical linear elasticity, to $r^{-3/2}$, with no need to take stretch gradients into consideration.

In this paper, the effects of strain rotation gradients on mode III crack propagation are investigated by performing an asymptotic analysis of the crack-tip fields derived from the flow theory of CS plasticity. It is expected that strain gradients become significant for $r < \ell$, where r is the distance from a crack-tip, and negligible for $r \gg \ell$, with a gradual transition in the intermediate region, where $r \approx \ell$. For the problem under consideration, a qualitative analysis shows that the leading order term of the velocity field turns out to be rotational, so that the leading order term of the strain rotation gradients does not vanish. The results show that the skew-symmetric stress field dominates the asymptotic field, due to the sole effect of the rotation gradients, and its singularity turns out to be much stronger than the stress singularity predicted by the classical J_2-flow theory. The increase specially occurs if the elastic strain gradients are kept sufficiently small, as the contribution of the elastic strain gradients strongly affects the asymptotic crack-tip fields, according to the results obtained for mode I crack propagation by Radi (2003).

The following notation is used throughout the paper. The components of a generic vector $\mathbf{v}$ or second order tensor $\mathbf{A}$ with respect to an orthogonal unit vectors basis $\{\mathbf{e}_i\}$ are defined as $v_i = \mathbf{v} \cdot \mathbf{e}_i$ and $A_{ij} = \mathbf{e}_i \cdot \mathbf{A}\mathbf{e}_j$, where a dot denotes the natural inner product of two vectors $\mathbf{a}$ and $\mathbf{b}$ or two second-order tensors $\mathbf{A}$ and $\mathbf{B}$. For any pair of vectors $\mathbf{a}$ and $\mathbf{b}$, the tensor product is defined by the identity $(\mathbf{a} \otimes \mathbf{b})\mathbf{u} = (\mathbf{u} \cdot \mathbf{b})\mathbf{a}$, which holds true for every vector $\mathbf{u}$. The deviatoric part of a generic second order tensor $\mathbf{A}$ is denoted by $\mathbf{A}^{\mathrm{D}}$, namely $\mathbf{A}^{\mathrm{D}} = \mathbf{A} - (\mathrm{tr}\,\mathbf{A}/3)\mathbf{I}$, where the prefix tr indicates the trace of a second order tensor and $\mathbf{I}$ is the second-order identity tensor. The symbols ∇, div and curl indicate the gradient, the divergence and the curl of a vector or tensor field, respectively, defined componentwise as $(\nabla \mathbf{v})_{ij} = \mathrm{v}_{i,j}$, $(\mathrm{div}\,\mathbf{A})_i = A_{ij,j}$ and $(\mathrm{curl}\,\mathbf{A})_{ij} = \varepsilon_{ikl} A_{jl,k}$, where ε_{ikl} is the third-order alternator and $(\,)_{,j}$ denotes the partial derivative with respect to the j-th spatial coordinate. Moreover, let $\mathbb{e}$ denote the third-order permutation tensor, defined as $(\mathbb{e}\mathbf{A})_i = \varepsilon_{ikl} A_{kl}$. A superimposed dot denotes a material time derivative. Finally, the MacAuley brackets $\langle\ \rangle$ define the function $\langle x \rangle = \frac{1}{2}(x + |x|)$, for every real value x.

2. Governing equations

The flow-theory version of the couple stress strain gradient plasticity (Fleck and Hutchinson, 1993), where SGs derive uniquely from rotation gradients, is adopted in this study. This model involves a single material length scale ℓ, which specifies the range where strain gradients are dominant and is generally of the order of few microns for ductile metals (Fleck et al., 1994).

The kinematic compatibility conditions between the displacement vector $\mathbf{u}$, rotation vector $\boldsymbol{\theta}$, strain tensor $\boldsymbol{\varepsilon}$ and deformation curvature tensor $\boldsymbol{\chi}$ are given by

$$\boldsymbol{\varepsilon}=\frac{1}{2}(\nabla\mathbf{u}+\nabla\mathbf{u}^{\mathrm{T}}),\quad \boldsymbol{\theta}=\frac{1}{2}curl\ \mathbf{u},\quad \boldsymbol{\chi}=curl\ \boldsymbol{\varepsilon}, \tag{2.1}$$

so that the tensor field $\boldsymbol{\chi}$ is irrotational.

According to the couple stress model (Toupin, 1962; Mindlin and Tiersten, 1962), the non-symmetrical Cauchy stress tensor $\mathbf{t}$ can be decomposed into a symmetric part $\boldsymbol{\sigma}$ and a skew-symmetric part $\boldsymbol{\tau}$, namely

$$\mathbf{t}=\boldsymbol{\sigma}+\boldsymbol{\tau}. \tag{2.2}$$

In addition, the couple stress tensor $\boldsymbol{\mu}$ is introduced as the work-conjugated quantity of $\boldsymbol{\chi}$. In the absence of body forces and body couples and for a smooth boundary, the principle of virtual work for a body B is given as (see Appendix)

$$\int_B(\boldsymbol{\sigma}\cdot\delta\boldsymbol{\varepsilon}+\boldsymbol{\mu}^{\mathrm{T}}\cdot\delta\boldsymbol{\chi})\mathrm{d}V=\int_{\partial B}(\mathbf{p}\cdot\delta\mathbf{u}+\mathbf{q}\cdot\delta\boldsymbol{\theta})\mathrm{d}S, \tag{2.3}$$

where the reduced surface traction vector $\mathbf{p}$ and couple stress traction vector $\mathbf{q}$ are, respectively,

$$\mathbf{p}=\mathbf{t}^{\mathrm{T}}\mathbf{n}+\frac{1}{2}\nabla\mu_{\mathrm{nn}}\times\mathbf{n},\quad \mathbf{q}=(\mathbf{I}-\mathbf{n}\otimes\mathbf{n})\boldsymbol{\mu}^{\mathrm{T}}\mathbf{n}, \tag{2.4}$$

with $\mathbf{n}$ denoting the outward unit normal. The principle of virtual work (2.3) provides the conditions of quasistatic equilibrium of forces and moments within the body (see Appendix), namely

$$\mathrm{div}\ \mathbf{t}^{\mathrm{T}}=\mathbf{0},\quad \mathrm{div}\boldsymbol{\mu}^{\mathrm{T}}+\mathbb{e}\boldsymbol{\tau}=\mathbf{0}, \tag{2.5}$$

respectively.

Within the context of small deformations incremental theory, the total strain rate $\dot{\boldsymbol{\varepsilon}}$ is the sum of elastic $\dot{\boldsymbol{\varepsilon}}^{\mathrm{e}}$ and plastic $\dot{\boldsymbol{\varepsilon}}^{\mathrm{p}}$ parts. Similarly, the total deformation curvature rate $\dot{\boldsymbol{\chi}}$ is the sum of elastic $\dot{\boldsymbol{\chi}}^{\mathrm{e}}$ and plastic $\dot{\boldsymbol{\chi}}^{\mathrm{p}}$ contributions. Both elastic parts are related to stress and couple stress rates through the incremental relations

$$\dot{\boldsymbol{\varepsilon}}^{\mathrm{e}}=\frac{1}{E}[(1+\nu)\dot{\boldsymbol{\sigma}}-\nu(\mathrm{tr}\dot{\boldsymbol{\sigma}})\mathbf{I}],\quad \dot{\boldsymbol{\chi}}^{\mathrm{eT}}=\frac{1+\nu}{E\ell_e^2}\dot{\boldsymbol{\mu}}, \tag{2.6}$$

where E is the elastic Young modulus, ν the Poisson ratio and ℓ_{e} the elastic length scale introduced by Fleck and Hutchinson (1993) in order to partition the deformation curvature rate tensor into its elastic part $\dot{\boldsymbol{\chi}}^{\mathrm{e}}$ and plastic part $\dot{\boldsymbol{\chi}}^{\mathrm{p}}$, with $\ell_{\mathrm{e}}<\ell$. It is worth noting that, within the couple stress theory $\boldsymbol{\mu}$, $\boldsymbol{\chi}$, $\boldsymbol{\chi}^{\mathrm{e}}$ and $\boldsymbol{\chi}^{\mathrm{p}}$ are purely deviatoric tensors.

The fundamental relationships of the constitutive model are briefly summarised below.

- Yield condition

$$f(\Sigma,Y)=\Sigma-Y=0, \tag{2.7}$$

where Σ is the overall effective stress, defined as

$$\Sigma = \sqrt{\frac{3}{2}\left(\boldsymbol{\sigma}^{\mathrm{D}} \cdot \boldsymbol{\sigma}^{\mathrm{D}} + \frac{\boldsymbol{\mu} \cdot \boldsymbol{\mu}}{\ell^2}\right)}, \tag{2.8}$$

and Y denotes the uniaxial flow stress defining isotropic hardening behaviour.

- Associative flow rules

$$\dot{\boldsymbol{\varepsilon}}^{\mathrm{p}} = \Lambda \frac{\partial f}{\partial \boldsymbol{\sigma}} = \frac{3}{2\Sigma} \Lambda \boldsymbol{\sigma}^{\mathrm{D}}, \quad \dot{\boldsymbol{\chi}}^{\mathrm{pT}} = \Lambda \frac{\partial \mathrm{f}}{\partial \boldsymbol{\mu}} = \frac{3}{2\Sigma\ell^2} \Lambda \boldsymbol{\mu}, \tag{2.9}$$

as follows from (2.7) and (2.8), where Λ is the plastic multiplier.

- Linear isotropic hardening rule

$$\dot{Y} = \Lambda H, \tag{2.10}$$

where $H = H(\Sigma)$ is the hardening modulus, defined, e.g., by a uniaxial tension test. In the following, linear isotropic hardening behaviour is considered, and hence the hardening modulus H is constant and may be defined as a function of the ratio $\alpha = E_{\mathrm{t}}/E (0 < \alpha < 1$ for pure hardening) between the tangent modulus and the elastic Young modulus for a bilinear stress–strain curve obtained by a uniaxial tension test, namely

$$H = \frac{\alpha}{1-\alpha} E. \tag{2.11}$$

- Prager consistency condition

$$\dot{f} = 0, \quad \Leftrightarrow \quad \dot{\Sigma} = \dot{Y},$$

which gives the non-negative plastic multiplier Λ as

$$\Lambda = \begin{cases} \langle \dot{\Sigma} \rangle / H & \text{if } f(\Sigma, Y) = 0 \\ 0 & \text{if } f(\Sigma, Y) < 0, \end{cases} \tag{2.12}$$

where

$$\dot{\Sigma} = \frac{3}{2\Sigma} (\boldsymbol{\sigma}^{\mathrm{D}} \cdot \dot{\boldsymbol{\sigma}} + \ell^{-2} \boldsymbol{\mu} \cdot \dot{\boldsymbol{\mu}}). \tag{2.13}$$

From (2.6) and (2.9), the elastic–plastic incremental constitutive equations for the stress and couple stress tensors, $\boldsymbol{\sigma}$ and $\boldsymbol{\mu}$, turn out to be

$$\dot{\boldsymbol{\varepsilon}} = \frac{1}{E}[(1+\nu)\dot{\boldsymbol{\sigma}} - \nu(\mathrm{tr}\ \dot{\boldsymbol{\sigma}})\mathbf{I}] + \frac{3}{2\Sigma} \Lambda \boldsymbol{\sigma}^{\mathrm{D}}, \tag{2.14}$$

$$\ell^2 \dot{\boldsymbol{\chi}}^{\mathrm{T}} = \frac{1+\nu}{E\xi^2} \dot{\boldsymbol{\mu}} + \frac{3}{2\Sigma} \Lambda \boldsymbol{\mu}, \tag{2.15}$$

where the non-dimensional parameter $\xi = \ell_{\mathrm{e}}/\ell < 1$ has been introduced. The constitutive equations (2.14) and (2.15) hold when the yield condition (2.7) is satisfied. If not, the plastic multiplier Λ is set equal to 0, so that isotropic elastic behaviour with couple stress is recovered. Therefore, strain gradient effects occur also for a purely elastic response. However, their magnitude may be made arbitrarily small by choosing a sufficiently small ξ ratio. Finally, note that the constitutive equations (2.14) and (2.15) reduce to the widely used J_2-flow theory of plasticity when the strain gradients are vanishing small.

3. Mode III crack propagation problem

3.1. Formulation of the problem for the crack-tip fields

We consider here the problem of a semi-infinite plane crack propagating at constant velocity V along a rectilinear path. Reference is made to a cylindrical coordinate system (r, θ, x_3) centred at the crack-tip and moving with it towards the $\theta = 0$ direction, where the x_3-axis coincides with the straight crack front. The condition of steady-state propagation yields the following time derivative rule for any arbitrary scalar function ϕ:

$$\dot{\phi} = \frac{V}{r}\left(\frac{\partial \phi}{\partial \theta}\sin\theta - r\frac{\partial \phi}{\partial r}\cos\theta\right), \tag{3.1}$$

which asymptotically holds also for not uniform, but quasi-static, crack propagation.

For antiplane problems, the non-vanishing stress and couple stress components, in polar coordinates, are σ_{r3}, $\sigma_{\theta 3}$, τ_{r3}, $\tau_{\theta 3}$, μ_{rr}, $\mu_{r\theta}$, $\mu_{\theta r}$ and $\mu_{\theta\theta}$, where $\mu_{\theta\theta} = -\mu_{rr}$. Accordingly, the strain and deformation curvature components are ε_{r3}, $\varepsilon_{\theta 3}$, $\chi_{\theta r}$, $\chi_{r\theta}$, χ_{rr}, and $\chi_{\theta\theta}$, where $\chi_{\theta\theta} = -\chi_{rr}$.

In a polar coordinate system, the conditions of equilibrium (2.5) become

$$\begin{aligned} &(r t_{r3})_{,r} + t_{\theta 3,\theta} = 0, \\ &(r\mu_{rr})_{,r} + \mu_{\theta r,\theta} - \mu_{\theta\theta} + 2r\tau_{\theta 3} = 0, \\ &(r\mu_{r\theta})_{,r} + \mu_{\theta\theta,\theta} + \mu_{\theta r} - 2r\tau_{r3} = 0, \end{aligned} \tag{3.2}$$

and the incremental form of the kinematic compatibility conditions $(2.1)_{1,3}$ become

$$2\dot{\varepsilon}_{r3} = v_{3,r}, \quad 2r\dot{\varepsilon}_{\theta 3} = v_{3,\theta}, \tag{3.3}$$

$$\dot{\chi}_{rr} = \dot{\varepsilon}_{3\theta,r}, \quad \dot{\chi}_{r\theta} = \dot{\varepsilon}_{3\theta,\theta} + \frac{\dot{\varepsilon}_{3\mathrm{r}}}{r}, \quad \dot{\chi}_{\theta r} = -\dot{\varepsilon}_{3r,r}. \tag{3.4}$$

Equations (3.2)–(3.4) together with the constitutive incremental Equations (2.10), (2.14) and (2.15) form a system of first order PDEs that governs the problem of the crack propagation. The asymptotic crack-tip fields are sought in a separable variable form, of the type $\phi(r, \theta) = r^{\rho} F(\theta)$, where ϕ is a generic function and ρ is the exponent which defines the asymptotic behaviour of ϕ as $r \to 0$. A qualitative analysis is first performed to obtain the relative order of singularity of the crack-tip fields. Consider that the symmetric part of the true stress behaves as $\boldsymbol{\sigma} = \mathrm{O}(r^s)$ as $r \to 0$. Then, the implications sketched in Box 1 can be established and the velocity, stress and couple stress asymptotic crack-tip fields are assumed in the following form

$$\begin{aligned} &v_3(r,\theta) = V\left(\frac{r}{R}\right)^s w(\theta), \quad \sigma_{\alpha 3}(r,\theta) = E\left(\frac{r}{R}\right)^s s_{\alpha}(\theta), \\ &\tau_{\alpha 3}(r,\theta) = E\frac{\ell^2}{r^2}\left(\frac{r}{R}\right)^s t_{\alpha}(\theta), \quad \mu_{\alpha\beta}(r,\theta) = E\frac{\ell^2}{r}\left(\frac{r}{R}\right)^s M_{\alpha\beta}(\theta), \end{aligned} \tag{3.5}$$

where the Greek indices α and β stand for polar coordinates r and θ. The exponent s defines the radial dependence of the symmetric stress and velocity fields, whereas the couple stress and skew symmetric stress fields behave as r^{s-1} and r^{s-2} as r

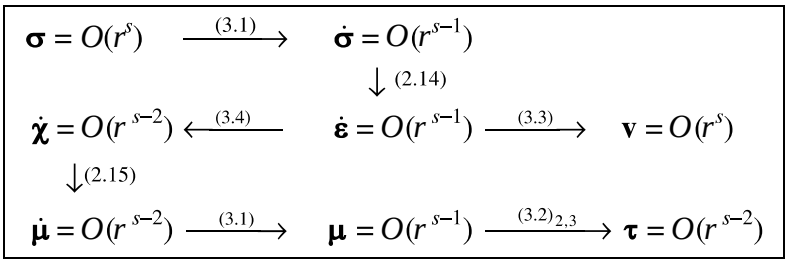

Box 1. Qualitative asymptotic analysis of crack-tip fields for mode III crack-propagation problem in couple stress solids.

approaches zero, respectively. The constant R is an undetermined amplitude factor of the leading order asymptotic fields. It is worth noting that the solution of the homogeneous asymptotic problem can be determined up to the amplitude factor R, which depends on far-field loading and specimen geometry and can be estimated by matching with the far-field conditions. However, the asymptotic analysis can capture the strength of the singularity of the stress field and couple stress, and the variation of the angular functions once a normalisation condition is adopted. Note also that, the following condition holds true:

$$M_{\theta\theta} = -M_{rr}, \tag{3.6}$$

as $\boldsymbol{\mu}$ and, thus, $\mathbf{M}$ are deviatoric tensors.

According to representations (3.5) of the stress and couple stress crack-tip fields the overall effective stress and flow stress fields near the crack-tip assume the following asymptotic expressions

$$\Sigma(r,\theta) = E\frac{\ell}{r}\left(\frac{r}{R}\right)^s \Gamma(\theta), \quad \Upsilon(r,\theta) = E\frac{\ell}{r}\left(\frac{r}{R}\right)^s \gamma(\theta), \tag{3.7}$$

respectively, where the definition of the function Γ follows from (2.8) and $(3.5)_{2,4}$ as

$$\Gamma = \sqrt{1.5\ \mathbf{M}\cdot\mathbf{M}}. \tag{3.8}$$

Therefore, only the couple stress field contributes to the most singular term of the effective stress and, thus, to the yield condition.

When the asymptotic fields (3.5) are introduced into equilibrium equations (3.2), by using (3.6), the following ODEs are derived at leading order

$$\begin{aligned} t_\theta' &= (1-s)t_r, \\ M_{\theta r}' &= -(1+s)M_{rr} - 2t_\theta, \\ M_{rr}' &= -M_{\theta r} + sM_{r\theta} - 2t_r, \end{aligned} \tag{3.9}$$

where $(\,)' = \mathrm{d}(\,)/\mathrm{d}\theta$.

By using the steady-state derivative (3.1), the rates of the fields $\boldsymbol{\sigma}$, $\boldsymbol{\mu}$ and Y in $(3.5)_{2,4}$ and (3.7) can be written in the form

$$\begin{aligned}
&\dot{\sigma}_{\alpha 3}(r,\theta) = E\frac{V}{r}\left(\frac{r}{R}\right)^{s} h_{\alpha}(\theta),\\
&\dot{\mu}_{\alpha\beta}(r,\theta) = EV\frac{\ell^2}{r^2}\left(\frac{r}{R}\right)^{s} H_{\alpha\beta}(\theta),\\
&\dot{Y}(r,\theta) = EV\frac{\ell}{r^2}\left(\frac{r}{R}\right)^{s} \kappa(\theta).
\end{aligned} \tag{3.10}$$

The cylindrical components of the vector $\mathbf{h}$ and tensor $\mathbf{H}$ introduced in $(3.10)_{1,2}$, which may be derived on application of (3.1) to the representation $(3.5)_{2,4}$ of the symmetric stress and couple stress field, respectively, are

$$h_r = (s_r' - s_\theta)\sin\theta - s s_r\cos\theta, \quad h_\theta = (s_\theta' + s_r)\sin\theta - s s_\theta\cos\theta, \tag{3.11}$$

and

$$\begin{aligned}
&H_{rr} = (M_{rr}' - M_{\theta r} - M_{r\theta})\sin\theta + (1-s)M_{rr}\cos\theta,\\
&H_{r_\theta} = (M_{r\theta}' + 2M_{rr})\sin\theta + (1-s)M_{r\theta}\cos\theta,\\
&H_{\theta r} = (1-s)(M_{rr}\sin\theta + M_{\theta r}\cos\theta) - 2t_\theta\sin\theta.
\end{aligned} \tag{3.12}$$

Note that $(3.9)_2$ has been used in the latter equation and the condition $H_{\theta\theta} = -H_{rr}$ holds as a consequence of (3.6). The definition of the function κ, introduced in $(3.10)_3$, follows from $(3.7)_2$ and (3.1) as

$$\kappa = \gamma'\sin\theta + (1-s)\gamma\cos\theta. \tag{3.13}$$

As sketched in Box 1, the strain and deformation curvature rates must have the same radial dependence assumed for the stress and couple stress rates in $(3.10)_{1,2}$. From (2.14)–(2.15), it turns out that

$$\dot{\varepsilon}_{\alpha 3}(r,\theta) = \frac{V}{r}\left(\frac{r}{R}\right)^{s} \mathrm{d}_{\alpha}(\theta), \quad \dot{\chi}_{\alpha\beta}(r,\theta) = \frac{V}{r^2}\left(\frac{r}{R}\right)^{s} X_{\alpha\beta}(\theta). \tag{3.14}$$

In contrast with the problems of a stationary (Xia and Hutchinson, 1996; Huang et al., 1997) or steadily propagating (Radi, 2003) crack under mode I or mode II loading conditions, the dominant strain rate field for the antiplane crack problem turns out to be rotational, so that the compatibility equations (3.4) admit non-vanishing deformation curvature rates at lowest order. By using the asymptotic representations $(3.5)_1$ and $(3.14)_1$ of the velocity and strain rate fields, the kinematic compatibility conditions (3.3) become

$$d_r = \frac{s}{2}w, \quad w' = 2\,d_\theta. \tag{3.15}$$

By introducing relations (3.14) and the algebraic condition $(3.15)_1$ into equations (3.4) it follows that

$$X_{rr} = (s-1)d_\theta, \quad X_{r\theta} = d_\theta' + \frac{s}{2}w, \quad X_{\theta r} = \frac{s}{2}(1-s)w. \tag{3.16}$$

As a consequence of the definitions (3.7) of the effective and flow stress fields, the yield condition (2.7) can be written as

$$\Gamma = \gamma. \tag{3.17}$$

By substituting the asymptotic fields (3.5)–(3.7) and their rates (3.10) and (3.14) in the incremental constitutive relationships (2.14), (2.15) and (2.10), the following set of equations is obtained

$$\mathbf{d} = (1+\nu)\mathbf{h} + \langle\lambda\rangle\mathbf{s}, \tag{3.18}$$

$$\mathbf{X}^{\mathrm{T}} = \frac{1+\nu}{\xi^2}\mathbf{H} + \langle\lambda\rangle\mathbf{M}, \tag{3.19}$$

$$\kappa = 2\langle\lambda\rangle h\Gamma/3, \tag{3.20}$$

where $h = H/E$ and λ is the normalised plastic multiplier, defined such that $\lambda = 0$ when $\Gamma < \gamma$, and

$$\lambda = \frac{1}{h}\left(\frac{3}{2\Gamma}\right)^2 \mathbf{M}\cdot\mathbf{H} \tag{3.21}$$

when $\Gamma = \gamma$, in agreement with (2.12) and (2.13).

Equations (3.18)–(3.20) hold true when the effective stress and flow stress fields obey the yield condition (3.17). During elastic unloading or neutral loading $\lambda \leq 0$, so that (3.18) and (3.19) reduce to the incremental equations of linear isotropic elasticity with strain gradient effects, and Equation (3.20) becomes equivalent to the condition $\dot{Y} = 0$.

3.2. Explicit form of the ODEs system

The explicit form of the ODEs system is now formulated by performing some manipulations on the equations established in the previous subsection. In particular the introduction of $(3.15)_1$ into (3.18) yields

$$(1+\nu)h_r + \langle\lambda\rangle s_r = \frac{s}{2}w, \quad (1+\nu)h_\theta + \langle\lambda\rangle s_\theta = d_\theta. \tag{3.22}$$

From Equations (3.16) and (3.19) the following relations are derived:

$$\begin{aligned}
&\frac{1+\nu}{\xi^2}H_{rr} + \langle\lambda\rangle M_{rr} = (s-1)d_\theta,\\
&\frac{1+\nu}{\xi^2}H_{r\theta} + \langle\lambda\rangle M_{r\theta} = \frac{s}{2}(1-s)w,\\
&d'_\theta = \frac{1+\nu}{\xi^2}H_{\theta r} + \langle\lambda\rangle M_{\theta r} - \frac{s}{2}w.
\end{aligned} \tag{3.23}$$

Equations $(3.23)_{1,2}$ can be rearranged by introducing the following expression of the plastic multiplier (3.21)

$$\lambda = \frac{1}{h}\left(\frac{3}{2\Gamma}\right)^2 (2M_{rr}H_{rr} + M_{r\theta}H_{r\theta} + M_{\theta r}H_{\theta r}), \tag{3.24}$$

to explicitly yield the functions H_{rr} and $H_{r\theta}$:

$$\begin{bmatrix} H_{rr} \\ H_{r\theta} \end{bmatrix} = \frac{1}{\Delta} \begin{bmatrix} h^* + M_{r\theta}^2 & -M_{r\theta} M_{rr} \\ -2M_{r\theta} M_{rr} & h^* + 2M_{rr}^2 \end{bmatrix} \begin{bmatrix} z_r \\ z_\theta \end{bmatrix}, \tag{3.25}$$

where

$$h^* = h \left(\frac{2\Gamma}{3} \right)^2 \frac{1+\nu}{\xi^2}, \quad \Delta = (h^* + 2M_{rr}^2 + 2M_{r\theta}^2) h^*, \tag{3.26}$$
$$z_\alpha = h \left(\frac{2\Gamma}{3} \right)^2 X_{\alpha r} - M_{r\alpha} M_{\theta r} H_{\theta r} \quad (\alpha = r, \theta),$$

being Δ always positive for positive strain-hardening.

Note that the expressions of H_{rr} and $H_{r\theta}$ given by (3.25) do not depend on the derivatives of the unknown angular functions, as follows from the definitions (3.26) and the algebraic expressions $(3.12)_3$ and $(3.16)_{1,3}$ for $H_{\theta r}$, X_{rr} and $X_{\theta r}$. Then, the explicit expressions (3.25) for H_{rr} and $H_{r\theta}$ together with the results $(3.12)_3$ for $H_{\theta r}$ can be introduced in (3.24) to obtain the normalised plastic multiplier λ in explicit form. Moreover, the derivatives with respect to the angular coordinate θ of the couple stress components M_{rr} and $M_{r\theta}$ can be obtained from $(3.12)_{1,2}$ in the form

$$\begin{aligned} M'_{rr} &= M_{\theta r} + M_{r\theta} - (1-s) M_{rr} \cot\theta + H_{rr} / \sin\theta, \\ M'_{r\theta} &= -2M_{rr} - (1-s) M_{r\theta} \cot\theta + H_{r\theta} / \sin\theta. \end{aligned} \tag{3.27}$$

Finally, from (3.11), it follows that

$$\begin{aligned} s'_r &= s_\theta + (h_r + s s_r \cos\theta) / \sin\theta, \\ s'_\theta &= -s_r + (h_\theta + s s_\theta \cos\theta) / \sin\theta, \end{aligned} \tag{3.28}$$

where h_r and h_θ can be found by (3.22). Similarly, from (3.13) and (3.20) one obtains

$$\gamma' = (s-1)\gamma \cot\theta + 2\langle\lambda\rangle h\Gamma / (3 \sin\theta). \tag{3.29}$$

Equations $(3.9)_{1,2}$, $(3.15)_2$, $(3.23)_3$, (3.27)–(3.29) form a system of nine first order and homogeneous ODEs governing the near-tip stress and velocity fields for the antiplane crack propagation problem in couple stress strain gradient solids. This system may be written in the following explicit form:

$$\mathbf{y}'(\theta) = \begin{cases} \mathbf{f}_{\mathrm{p}}(\theta, \mathbf{y}(\theta)) & \text{if } \Gamma = \gamma \text{ and } \lambda > 0, \\ \mathbf{f}_{\mathrm{e}}(\theta, \mathbf{y}(\theta)) & \text{if } \Gamma < \gamma \text{ or } (\Gamma = \gamma \text{ and } \lambda \leq 0), \end{cases} \tag{3.30}$$

where the vector $\mathbf{y}$ collects the nine unknown angular functions, i.e.,

$$\mathbf{y} = \{w, t_\theta, s_r, s_\theta, M_{rr}, M_{r\theta}, M_{\theta r}, d_\theta, \gamma\}. \tag{3.31}$$

Note that t_r and d_r have not been considered as primary unknown functions because the former may be obtained from $(3.9)_3$, by using (3.6) and $(3.27)_1$, whereas the latter is given by the algebraic equation $(3.15)_1$ once all the functions in $\mathbf{y}$ are known.

The unknown exponent s can be determined as an eigenvalue of the non-linear homogeneous problem (3.30), once a normalisation condition is assumed for the asymptotic solution.

The position of a material point moving along a rectilinear path with respect to the crack-tip is specified by the angular coordinate θ. A generic material point near the trajectory of the crack-tip experiences plastic loading ahead of the crack-tip, elastic unloading at $\theta=\theta_1$, and subsequent plastic reloading at $\theta=\theta_2$. The elastic unloading angle θ_1 is defined by the condition $\dot{\Sigma}=0$, which occurs for $\lambda(\theta_1)=0$. Plastic reloading on crack flanks occurs at the angular coordinate θ_2, where the material point reaches a stress state satisfying the yield condition (3.17) again.

The velocity field $(3.5)_1$ can be integrated to obtain the displacement field $u_3(r,\theta)$ in the vicinity of the crack-tip. Consider the following asymptotic behaviour for $u_3(r,\theta)$:

$$u_3(r,\theta)=r\left(\frac{r}{R}\right)^s u(\theta), \tag{3.32}$$

consistent with $(3.5)_1$, since $\dot{u}_3=v_3$. Then, the use of the steady-state condition (3.1) yields the following first order ODE

$$u'=\frac{1}{\sin\theta}\left[w+(s+1)u\cos\theta\right], \tag{3.33}$$

which can be numerically solved for $u(\theta)$ after (3.30).

4. Mode III boundary conditions

The condition of Mode III crack propagation restricts the analysis to the interval $0\leq\theta\leq\pi$. It is reasonable to assume regular behaviour of the angular functions at $\theta=0$, so that relations (3.11)–(3.13) lead to

$$\mathbf{h}(0)=-s\mathbf{s}(0),\quad \mathbf{H}(0)=(1-s)\mathbf{M}(0),\quad \kappa(0)=(1-s)\gamma(0). \tag{4.1}$$

The skew-symmetry of the antiplane crack problem requires along the plane at $\theta=0$ ahead of the crack-tip

$$u(0)=0,\quad w(0)=0,\quad M_{\theta r}(0)=0, \tag{4.2}$$

which imply by $(3.22)_1$, $(3.23)_{2,3}$ and $(4.1)_{1,2}$

$$s_r(0)=M_{r\theta}(0)=d'_\theta(0)=0. \tag{4.3}$$

By using condition $(4.1)_2$, the normalised plastic multiplier (3.21) at $\theta=0$ results in

$$\lambda(0)=\frac{3}{2h}(1-s)>0. \tag{4.4}$$

The introduction of relations $(4.1)_{1,2}$ and (4.4) into the constitutive equations $(3.22)_2$ and $(3.23)_1$ evaluated at $\theta=0$, after some algebraic manipulations, yields

$$d_\theta(0)=[\lambda(0)-s(1+\nu)]s_\theta(0),\quad M_{rr}(0)=-\frac{2h\xi^2 d_\theta(0)}{2h(1+\nu)+3\xi^2}. \tag{4.5}$$

The vanishing of the radial traction at $\theta = 0$ requires

$$t_{r3} - \frac{1}{2r}\mu_{rr,\theta} = 0, \tag{4.6}$$

which implies

$$M'_{rr}(0) = 2t_r(0). \tag{4.7}$$

Hence, from (4.7) and the equilibrium condition $(3.9)_3$ it turns out that

$$t_r(0) = 0, \quad M'_{rr}(0) = 0. \tag{4.8}$$

In order to solve the system (3.30), the Runge–Kutta procedure is used (subroutine DIVPRK of the IMSL library). This approach requires knowledge of the initial values $\mathbf{y}(0)$. Since all the assigned boundary conditions (4.2), (4.3), (4.5) and (4.8) are homogeneous, the normalisation condition for the stress field

$$s_\theta(0) = 1 \tag{4.9}$$

is adopted to avoid the trivial solution.

Under the hypothesis that the zone ahead of the crack-tip is experiencing plastic loading, the yield condition $\gamma(0) = \Gamma(0)$ holds true, where $\Gamma(0)$ may be obtained by using conditions (3.6), $(4.2)_3$, $(4.3)_2$ in (3.8), so that

$$\gamma(0) = \sqrt{3M^2_{rr}(0)}. \tag{4.10}$$

The vanishing of the general tractions (2.3)–(2.4) on the crack surfaces requires

$$t_{\theta 3} + \frac{1}{2}\mu_{\theta\theta,r} = 0, \quad \mu_{\theta r} = 0, \tag{4.11}$$

which implies the following two boundary conditions at $\theta = \pi$ for the system (3.30)

$$2t_\theta(\pi) + (1-s)M_{rr}(\pi) = 0, \quad M_{\theta r}(\pi) = 0. \tag{4.12}$$

By taking the derivatives with respect to θ of $(3.22)_1$ and $(3.11)_1$, evaluated at $\theta = 0$, the following result can be found by using $(4.5)_1$

$$s'_r(0) = \left[s + \frac{2h(1+\nu)}{3+2h(1+\nu)} \right] s_\theta(0). \tag{4.13}$$

Similarly, by using the derivatives of $(3.12)_2$ and $(3.23)_2$ evaluated at $\theta = 0$, it may be found that

$$M'_{r\theta}(0) = \frac{\xi^2 s(1-s)d_\theta(0) - 2(1+\nu)M_{rr}(0)}{(1+\nu)(2-s) + \xi^2\lambda(0)}. \tag{4.14}$$

When the equilibrium equation $(3.9)_1$ is evaluated at $\theta = 0$ we get

$$t'_\theta(0) = (1-s)t_r(0). \tag{4.15}$$

The value of $\gamma'(0)$ can be obtained by taking the derivative of $\Gamma(\theta)$ from (3.8) and by substituting for the stress and couple stress components evaluated at $\theta = 0$ from $(4.2)_3$, and (4.9). After a lengthy but straightforward calculation, one obtains

$$\gamma'(0) = 0. \tag{4.16}$$

Finally, differentiation of (3.33) and use of $(3.15)_2$ yield

$$u'(0) = -2d_\theta(0)/s. \tag{4.17}$$

The initial conditions (4.2), $(4.3)_{1,2}$, (4.5), $(4.8)_1$, (4.9) and (4.10) give the values of all the unknown functions at $\theta = 0$ depending on s and $t_\theta(0)$. These two unknown initial values can be calculated by an iterative procedure based on the achievement of the two boundary conditions (4.12) at $\theta = \pi$. This iteration is performed by using the modified Powell hybrid method (subroutine DNEQNF of the IMSL library), until the conditions (4.12) on the general tractions are verified within a prescribed accuracy.

The numerical integration procedure of the governing ODE system (3.30) displays a numerical difficulty at $\theta = 0$, due to the term $\sin\theta$ which multiplies the highest order derivative. This inconvenience can be bypassed by performing a Taylor series expansions of the unknown angular functions collected in the vector $\mathbf{y}$, starting at $\theta = 0$, namely:

$$\mathbf{y}(\varepsilon) = \mathbf{y}(0) + \varepsilon\mathbf{y}'(0) + \mathrm{o}(\varepsilon), \tag{4.18}$$

where $\varepsilon \ll 1$. In this way, the unknown functions can be evaluated at $\theta = \varepsilon$, since the values of the unknown functions and their derivatives at $\theta = 0$ are known from symmetry conditions and relations $(4.3)_3$, (4.7), $(4.8)_2$, (4.13)–(4.16). Once that $\mathbf{y}(\varepsilon)$ has been determined by (4.18) within an error lower than ε, the numerical integration of (3.30) can be performed by starting at $\theta = \varepsilon$, rather than at $\theta = 0$. A similar strategy must be applied to (3.33) adopting (4.17).

5. Results

In the following, results for a fixed value of the Poisson ratio ($\nu = 0.3$) are reported. Note that they are meaningful within the range $r < \ell$.

The variation of the exponent s with the characteristic lengths ratio $\xi = \ell_e/\ell$ and with the hardening parameter α is plotted in Figures 1a and 1b, respectively. It is found that s ranges between 0.5 and 1, which means that even if the symmetric stress components are not singular at the crack-tip, the couple stress and, principally, the skew-symmetric stress fields display strong singularities, respectively of the order of $s - 1$ and $s - 2$ according to (3.5). Although the skew-symmetric stresses dominate the asymptotic solution, only the couple stress field contributes to the effective stress Σ and to the strain-energy density, so that the high stress singularity does not violate the boundedness of the flux of energy toward the crack-tip. As the ratio ξ decreases and tends to vanish, the exponent s decreases and tends to 0.5 independently of the hardening coefficient α. It follows that the strength of the stress singularity increases with respect to the classical J_2-flow theory investigated by Ponte Castañeda (1987), also for small strain-hardening, due to the contribution of

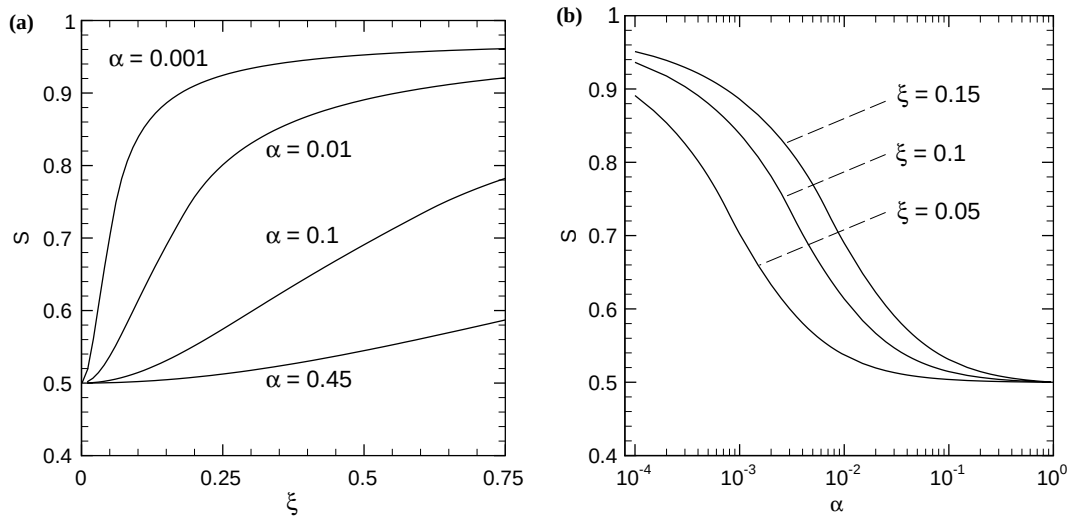

Figure 1. Exponent of the stress fields s as functions of the characteristic lengths ratio $\xi = \ell_e/\ell$ (*a*), and in terms of the hardening parameter α (*b*), Both plots are for $\nu = 0.3$.

the skew-symmetric stress component. In fact, the solution obtained by this Author for conventional elastic–plastic response predicts a weak stress singularity for small strain-hardening in agreement with the perfectly plastic limit behaviour of the material. As clearly shown in Figure 1a, for small values of the hardening parameter α the ratio ξ has a strong influence on the exponent s, whereas for the limiting case $\alpha \to 1$ the value of s is equal to 0.5 independently of ξ.

As $\xi \to 0$ the results of the present analysis approach those obtained for large strain-hardening, namely for $\alpha \to 1$ or equivalently $h \to \infty$. In both cases, in fact, the exponent s and the unloading angle θ approach the values 0.5 and 95.6°, respectively. Moreover, the angular variation of the couple stress field is quite close to the solution for elastic materials with strain gradient effects found by Zhang et al. (1998). However, as ξ tends to vanish the magnitude of the couple stress tends to reduce with respect to the (symmetric) stress components. This behaviour may be due to the role played by the ratio h/ξ^2 which appears in $(3.26)_1$ and becomes unbounded as $\xi \to 0$ or $h \to \infty$. Therefore, the vanishing of ξ and the increase of strain hardening modulus h produce quite similar effects, namely an increase of the tractions ahead of the crack-tip.

However, for $\xi = \ell_e/\ell = 0$ the leading order equations considered in Section 3 lose their physical meaning, since the constitutive equations tend to recover the classical J_2-flow theory. In this case, the elastic constitutive relation $(2.6)_2$ implies the vanishing of the couple stress fields $\boldsymbol{\mu}$, so that the non-symmetric stress field $\boldsymbol{\tau}$ must also vanish in order to satisfy the equilibrium equations $(2.5)_2$. Therefore, the overall effective stress entering the yield condition (2.7) reduce to

$$\Sigma = \sqrt{1.5\boldsymbol{\sigma}^{\mathrm{D}} \cdot \boldsymbol{\sigma}^{\mathrm{D}}}, \tag{5.1}$$

in agreement with the classical von Mises yield condition. Correspondingly, the constitutive rate relation (2.14), the equilibrium equations $(2.5)_1$ and the compatibility condition $(2.1)_1$ recover the classical J_2-flow theory. In this case, the leading order

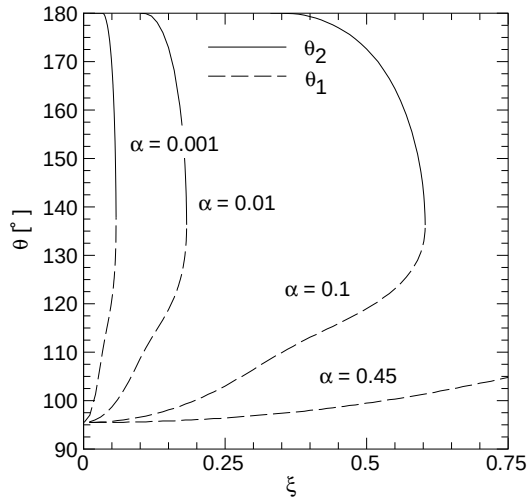

Figure 2. Elastic unloading (θ_1) and plastic reloading (θ_2) angles as functions of the ratio ξ, for $\nu = 0.3$.

term of the stress field under mode III loading conditions display a singularity s ranging between 0 and -0.5 depending on the hardening coefficient α (see Ponte Castañeda, 1987). However, as $\xi \to 0$ the asymptotic equations obtained in Section 3 do not recover these obtained by Ponte Castañeda (1987) for the classical J_2-flow theory, because the leading order term of the overall effective stress Σ, defined in $(3.7)_1$ and (3.8), does not reduce to the expression (5.1) which holds for the classical J_2-flow theory.

In Figure 1b, only small values of ξ ($\xi = 0.05, 0.1, 0.15$) are considered. As noted by Fleck and Hutchinson (1993), the adopted constitutive model may give reasonable predictions for $\xi \ll 1$ because the magnitude of the couple stress in the elastic sector results as being proportional to ξ^2 by $(2.6)_2$. As the strain gradient effects are associated with the occurrence of geometrically necessary dislocations (Gao and Huang, 2003), they scarcely influence the elastic behaviour. Therefore, the results obtained for small values of ξ are expected to be more realistic.

The variation of the elastic unloading and reloading angles, θ_1 and θ_2, with ξ is then reported in Figure 2. As ξ tends to vanish, an elastic unloading sector starts at $\theta_1 \approx 95.6^\circ$ and extends up to the crack flanks. Plastic reloading sectors appear for $\xi \geq 0.033$, $\xi \geq 0.1$ and $\xi \geq 0.33$ for $\alpha = 0.001$, 0.01 and 0.1, respectively. In every case, the size of the elastic unloading sector rapidly reduces and tends to vanish, respectively, for $\xi_p \cong 0.057$, $\xi_p \cong 0.18$ and $\xi_p \cong 0.6$. For $\xi > \xi_p$ the crack-tip zone is fully plastic. Again, as $\alpha \to 1$, the elastic unloading angle θ_1 turns out to be independent of ξ. The occurrence of an elastic unloading sector extending up to the crack-tip, as observed for the case of classical J_2-flow theory, is no longer predicted for some combinations of ξ and α, a finding also attained by Wei and Hutchinson (1997) in their numerical simulations. This result and the analysis of the elastic and plastic contributions to the total curvature rate (2.15) lead to the conclusion that the range of ξ corresponding to which the theory may give more realistic results depends on α for linear hardening material.

In Figure 3, the angular distributions of the asymptotic crack-tip fields are plotted for $\alpha = 0.001$, $\xi = 0.1$ (crack-tip zone fully plastic). All functions are normalised

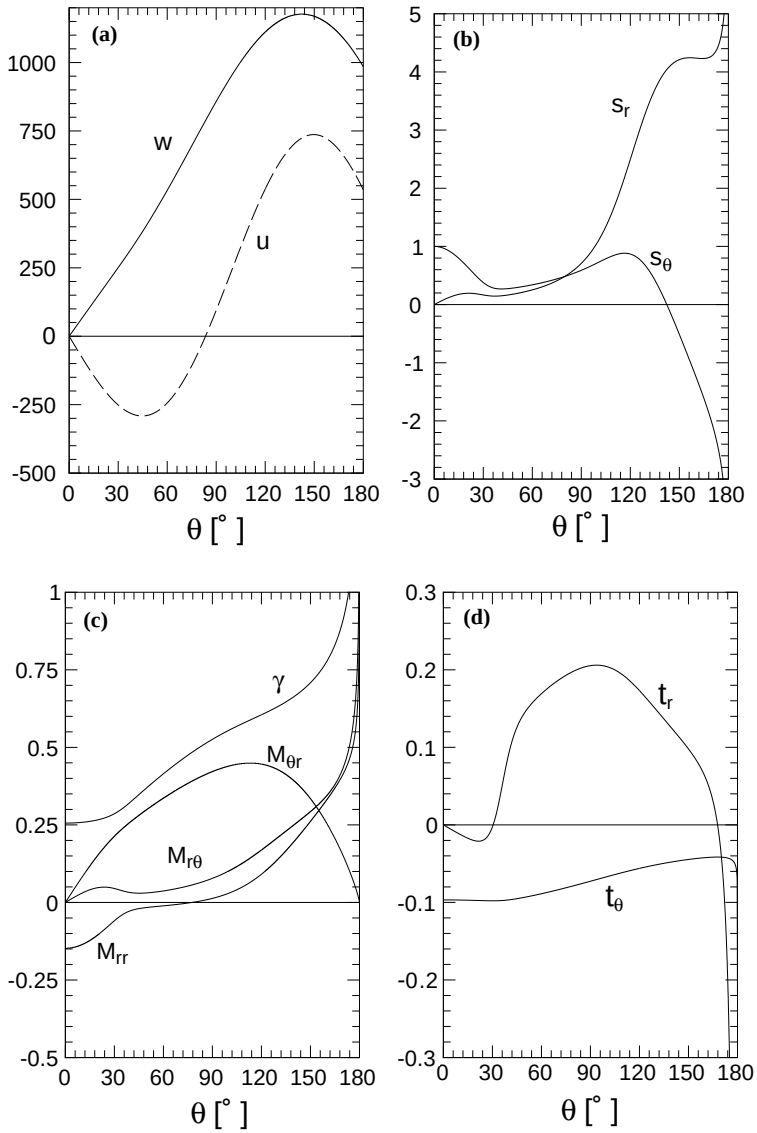

Figure 3. Angular variations of the asymptotic crack-tip fields of velocity and displacement (dashed curve) (a), symmetric stress (b), couple stress (c) and skew-symmetric stress (d) for $\nu = 0.3$, $\alpha = 0.001$ and $\xi = 0.1$.

by condition (4.9). In detail, in Figure 3a the angular variation of the out-of-plane velocity, w, and of the displacement field near the crack-tip, u, are reported. Differently from the classical solution of mode III crack-tip fields in linear strain-hardening materials obtained by Ponte Castañeda (1987), the present investigation shows that the displacements ahead of the crack-tip, namely for $0^\circ < \theta < 83.4^\circ$, and on the crack surface, at $\theta = 180^\circ$, turn out to be opposite in sign. Similar results have been also obtained by Zhang et al. (1998) for a stationary mode III crack in couple stress elasticity. This unusual aspect seems to be due to the presence of microstructure (grain, particles) introduced through the characteristic length ℓ. As noted by Yavari et al. (2002), during crack growth the separation process between two material particles at

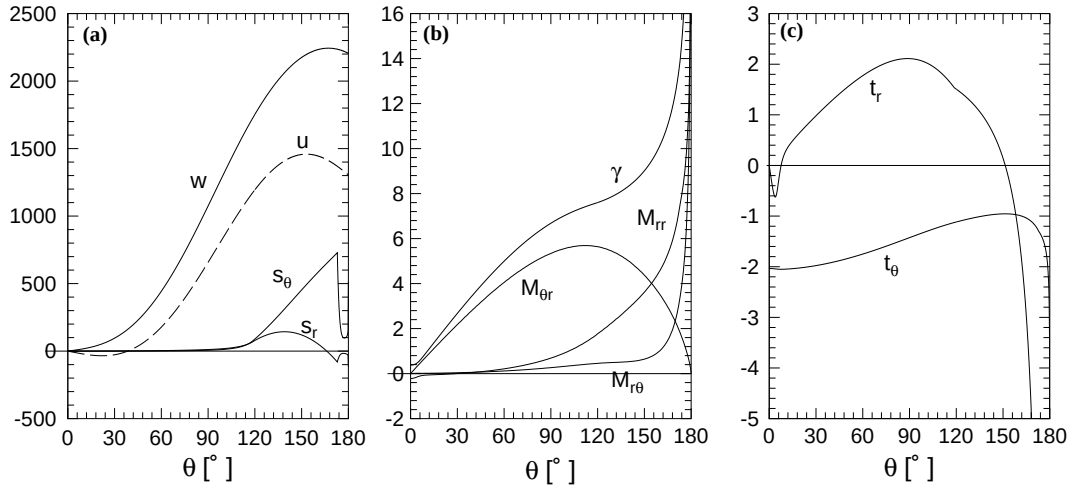

Figure 4. Angular variations of the asymptotic crack-tip fields of velocity, displacement (dashed curve) and symmetric stress (a), couple stress (b) and skew-symmetric stress (c) for $\nu = 0.3$, $\alpha = 0.01$ and $\xi = 0.15$.

the crack-tip can be divided into two steps: in the first step the particles rotate with respect to each other but do not move; in the second step they experience translation. The local rotation of grains and particles currently at the crack-tip produces opposite displacements ahead and behind the crack-tip under mode III loading condition creating a *scissors* effect. This is a further evidence that strain gradients considerably affect the solutions of fracture mechanics problems.

In Figure 3b the symmetric stress components s_r and s_θ are sketched, while in Figure 3c the angular variations of the couple stress field **M** and the current flow stress γ are reported. Note that the current flow stress, which is given by the single contribution from the couple stress field, rapidly increases at the crack flanks, in agreement with the solution obtained for crack propagation problems in elastic–plastic materials displaying linear isotropic strain-hardening (Ponte Castañeda, 1987).

The angular variations of the skew-symmetric stress components are plotted in Figure 3d. According to the inversion of the displacement field ahead of the crack-tip, therein the shear stress t_θ is negative and, thus, opposite to its counterpart in the mode III solution for classical J_2-flow theory (Ponte Castañeda, 1987). Also the radial shear stress component t_r displays negative values in a small sector ahead of the crack-tip. This switch in the shear directions agrees with the findings of Zhang et al. (1998). In addition, note that t_θ and M_{rr} tend to opposite values on the crack faces at $\theta = 180^\circ$, as required by the boundary condition $(4.12)_1$.

In Figure 4 the same quantities are displayed for $\alpha = 0.01$, $\xi = 0.15\,(\theta_1 = 118.9^\circ, \theta_2 = 172.8^\circ)$. Differently form the previous case, elastic unloading and plastic reloading sectors are present around the crack-tip with the effect of increasing considerably the magnitude of the symmetric stress components s_r and s_θ within the elastic unloading sector. Moreover, the negative displacement occurs in a smaller asymptotic sector $(0^\circ < \theta < 38.4^\circ)$ (Figure 4a) than that in Figure 3.

The plots in Figure 5 are for $\alpha = 0.1$, $\xi = 0.1\,(\theta_1 = 96.6^\circ)$. In this case, the plastic reloading sector is absent. As a consequence the function s_r increases almost line-

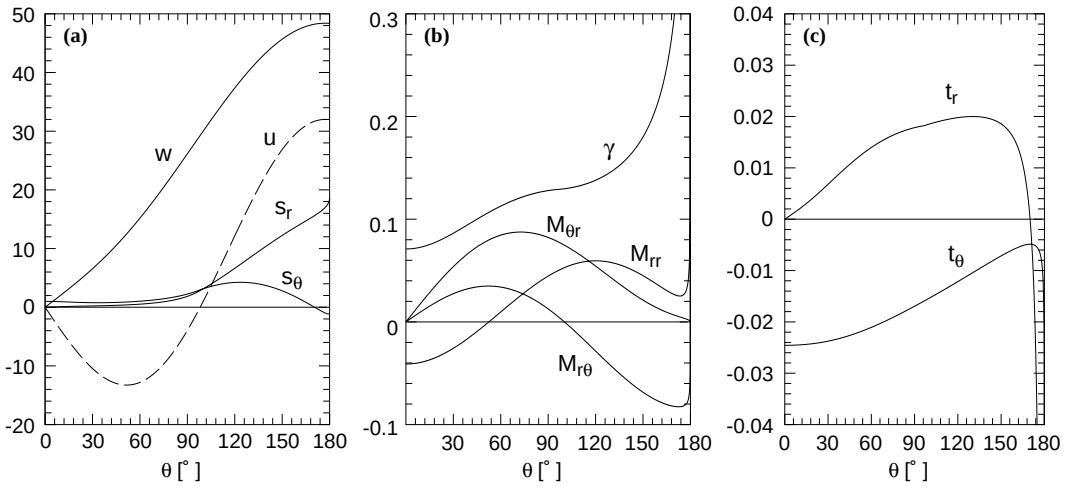

Figure 5. Angular variations of the asymptotic crack-tip fields of velocity, displacement (dashed curve) and symmetric stress (a), couple stress (b) and skew-symmetric stress (c) for $\nu = 0.3$, $\alpha = 0.1$ and $\xi = 0.1$.

arly in the elastic unloading zone up to the crack surfaces, whereas s_θ remains much smaller than s_r. The sector where the displacement is negative extends up to $\theta = 98.3^\circ$. The function t_θ is negative again, but t_r does not take negative values ahead of the crack-tip.

6. Conclusions

In this paper we performed an asymptotic analysis of the near-tip fields of a crack steadily propagating under mode III loading conditions, in a linear hardening elastic–plastic solid with strain gradient effects, modelled through the couple stress plasticity theory proposed by Fleck and Hutchinson (1993). This model incorporates a characteristic length ℓ in order to account for the size effect at the micron scale (ℓ is of the order of few microns for most ductile metals), together with an artificial elastic length scale ℓ_e introduced in order to partition the curvature rate into elastic and plastic contributions. Recently, other more sophisticated strain gradient theories have been proposed (SG theory, Fleck and Hutchinson, 1997; MSG theory, Gao et al., 1999), but an asymptotic analysis cannot be performed for those. In the case of SG theory, such investigation may give physically unacceptable results (see Chen et al., 1999, for mode I loading condition), while Shi et al. (2000) have shown that for an MSG solid the crack-tip fields do not admit a separable-variable form.

The main conclusions can be summarised as follows:

- the skew-symmetric stress field dominates the asymptotic solutions and its singularity is always stronger than square root, also for low strain hardening;
- the couple stress field displays a singularity weaker than square root, whereas the symmetric stress field turns out to be not singular;
- the ratio $\xi = \ell_e/\ell$ considerably affects the value of singularity, specially for low strain hardening: more singular solutions are achieved for $\xi \ll 1$. This is the suggested order of magnitude of ξ for real problems, based on dislocation mechanics (Wei and Hutchinson, 1997);

- the sign of the displacement field ahead of the crack-tip is found to be opposite to that on the crack face. This effect becomes more pronounced as the hardening coefficient increases and confirms the findings of Zhang et al. (1998) for a strain-gradient elastic material;
- an elastic unloading sector may occur, depending on the values of α and ξ.

The obtained results show that the use of the strain gradient plasticity model for the analysis of the stress field in the vicinity of a mode III propagating crack-tip gives more realistic predictions on the level of traction ahead of the crack-tip then the classical solution obtained for the J_2-flow theory, allowing the detailed mechanisms by which fracture may grow and propagate in ductile metals to be understood in more depth.

Acknowledgements

Financial support from University of Modena and Reggio Emilia is gratefully acknowledged.

Appendix

Boundary conditions and equilibrium equations for couple stress solids can be obtained from the principle of virtual work. We consider only the case where body forces and body couples are absent and the boundary ∂B of the body B is smooth, so that the outward unit normal $\mathbf{n}$ is always defined.

In terms of a virtual displacement fields $\delta\mathbf{u}$, virtual rotations $\delta\boldsymbol{\theta}$ and virtual curvatures $\delta\boldsymbol{\chi}$ are given respectively by

$$\delta\boldsymbol{\theta}=\frac{1}{2}curl\,\delta\mathbf{u},\quad \delta\boldsymbol{\chi}=\nabla\delta\boldsymbol{\theta}, \tag{A.1}$$

so that the corresponding deformation field takes the form

$$\delta\boldsymbol{\varepsilon}=\nabla\delta\mathbf{u}+\mathbb{e}\,\delta\boldsymbol{\theta}. \tag{A.2}$$

The expression of the internal virtual work (IVW), namely

$$\mathrm{IVW}=\int_B(\boldsymbol{\sigma}\cdot\delta\boldsymbol{\varepsilon}+\boldsymbol{\mu}^{\mathrm{T}}\cdot\delta\boldsymbol{\chi})\mathrm{d}V, \tag{A.3}$$

can be rearranged by using (A.1), (A.2) and the divergence theorem, to give

$$\mathrm{IVW}=\int_B[(\mathbb{e}\mathbf{t}^{\mathrm{T}}-div\boldsymbol{\mu}^{\mathrm{T}})\cdot\delta\boldsymbol{\theta}-(div\,\mathbf{t}^{\mathrm{T}})\cdot\delta\mathbf{u}]\mathrm{d}V+\int_{\partial B}(\mathbf{t}^{\mathrm{T}}\mathbf{n}\cdot\delta\mathbf{u}+\boldsymbol{\mu}^{\mathrm{T}}\mathbf{n}\cdot\delta\boldsymbol{\theta})\mathrm{d}S. \tag{A.4}$$

As IVW equates the external virtual work (EVW) the terms in parentheses in the volume integral must vanish, thus providing the equilibrium equations (2.5). The boundary conditions can not be deduced directly from the surface integral in (A.4) because $\delta\boldsymbol{\theta}$ is not independent of $\delta\mathbf{u}$. In order to obtain the correct form of the boundary conditions $\delta\boldsymbol{\theta}$ is decomposed in its normal ($\delta\boldsymbol{\theta}_n$) and tangential ($\delta\boldsymbol{\theta}_t$) components, i.e., $\delta\boldsymbol{\theta}=\delta\boldsymbol{\theta}_n+\delta\boldsymbol{\theta}_t$, where

$$\delta\boldsymbol{\theta}_n=(\delta\boldsymbol{\theta}\cdot\mathbf{n})\mathbf{n},\quad \delta\boldsymbol{\theta}_t=(\mathbf{I}-\mathbf{n}\otimes\mathbf{n})\delta\boldsymbol{\theta}. \tag{A.5}$$

As a consequence, the surface integral in (A.4) transforms to

$$\int_{\partial B} [\mathbf{t}^{\mathrm{T}}\mathbf{n}\cdot\delta\mathbf{u} + \mu_{\mathrm{nn}}\delta\boldsymbol{\theta}\cdot\mathbf{n} + (\mathbf{I}-\mathbf{n}\otimes\mathbf{n})\boldsymbol{\mu}^{\mathrm{T}}\mathbf{n}\cdot\delta\boldsymbol{\theta}]\mathrm{d}S. \tag{A.6}$$

Since $\delta\boldsymbol{\theta} = \frac{1}{2}curl\,\delta\mathbf{u}$, the second term in (A.6) can be transformed invoking twice the divergence theorem, yielding the following expression for the external virtual work

$$\mathrm{EVW} = \int_{\partial B} [(\mathbf{t}^{\mathrm{T}}\mathbf{n} + \frac{1}{2}\nabla\mu_{\mathrm{nn}}\times\mathbf{n})\cdot\delta\mathbf{u} + (\mathbf{I}-\mathbf{n}\otimes\mathbf{n})\boldsymbol{\mu}^{\mathrm{T}}\mathbf{n}\cdot\delta\boldsymbol{\theta}]\mathrm{d}S. \tag{A.7}$$

For antiplane shear $\delta\mathbf{u} = \delta V_3\mathbf{e}_3$; in addition $\mathbf{n} = \mathbf{e}_\theta$ on the crack face at $\theta = \pi$, so that the boundary conditions which must be imposed therein due to the vanishing of the general traction are given by (4.11).

References

Acharya, A. and Bassani, J.L. (2000). Lattice incompatibility and a gradient theory of crystal plasticity. *Journal of the Mechanics and Physics of Solids* **48**, 1565–1595.

Aifantis, E.C. (1984). On the microstructural origin of certain inelastic models. *Journal of Engineering Materials and Technology* **106**, 326–330.

Amazigo, J. and Hutchinson, J.W. (1977). Crack-tip fields in steady crack-growth with linear strain hardening. *Journal of the Mechanics and Physics of Solids* **25**, 81–97.

Bigoni, D. and Radi, E. (1996). Asymptotic solution for Mode III crack growth in J_2-elastoplasticity with mixed isotropic-kinematic strain hardening. *International Journal of Fracture* **77**, 77–93.

Chen, J.Y., Wei, Y., Huang, Y., Hutchinson, J.W. and Hwang, K.C. (1999). The crack-tip fields in strain gradient plasticity: the asymptotic and numerical analyses. *Engineering Fracture Mechanics* **64**, 625–648.

Chen, S.H. and Wang, T.C. (2002). A new deformation theory with strain gradient effects. *International Journal of Plasticity* **18**, 971–995.

Elssner, G., Korn, D. and Ruehle, M. (1994). The influence of interface impurities on fracture energy of UHV diffusion bonded metal-ceramic bicrystals. *Scripta Metallurgica et Materialia* **31**, 1037–1042.

Fannjiang, A.C., Chan, Y.-S. and Paulino, G.H. (2002). Strain gradient elasticity for antiplane shear cracks: a hypersingular integrodifferential equation approach. *SIAM Journal of Applied Mathematics* **62**, 1066–1091.

Fleck, N.A. and Hutchinson, J.W. (1993). A phenomenological theory for strain gradient effects in plasticity. *Journal of the Mechanics and Physics of Solids* **41**, 1825–1857.

Fleck, N.A., Muller, G.M., Ashby, M.F. and Hutchinson, J.W. (1994). Strain gradient plasticity: theory and experiment. *Acta Metallurgica et Materialia* **42**, 475–487.

Fleck, N.A. and Hutchinson, J.W. (1997). Strain gradient plasticity. In Advances in applied mechanics (Edited by J.W. Hutchinson and T.Y. Wu), Vol. 33. Academic Press, New York, pp. 295–361.

Fleck, N.A. and Hutchinson, J.W. (2001). A reformulation of strain gradient plasticity. *Journal of the Mechanics and Physics of Solids* **49**, 2245–2271.

Gao, H., Huang, Y., Nix, W.D. and Hutchinson, J.W. (1999). Mechanism-based strain gradient plasticity-I. Theory. *Journal of the Mechanics and Physics of Solids* **47**, 1239–1263.

Gao, H. and Huang, Y. (2003). Geometrically necessary dislocation and size dependent plasticity. *Scripta Materialia* **48**, 113–118.

Georgiadis, H.G. (2003). The mode III crack problem in microstructured solids governed by dipolar elasticity: static and dynamics analysis. *Journal of Applied Mechanics* **70**, 517–530.

Huang, Y., Zhang, L., Guo, T.F. and Hwang, K.C. (1997). Mixed mode near-tip fields for crack in materials with strain-gradient effects. *Journal of the Mechanics and Physics of Solids* **45**, 439–465.

Huang, Y., Chen, J.Y., Guo, T.F., Zhang, L. and Huang, K.C. (1999). Analytic and numerical studies on mode I and mode II fracture in elastic-plastic materials with strain gradient effects. *International Journal of Fracture* **100**, 1–27.

Hutchinson, J.W. (2000). Plasticity at the micron scale. *International Journal of Solids and Structures* **37**, 225–238.

Jiang, H., Huang, Y., Zhuang, Z. and Hwang, K.C. (2001). Fracture in mechanism-based strain gradient plasticity. *Journal of the Mechanics and Physics of Solids* **49**, 979–993.

Mindlin, R.D. (1965). Second gradient of strain and surface tension in linear elasticity. *International Journal of Solids and Structures* **1**, 417–438.

Mindlin, R.D. and Tiersten, H.F. (1962). Effects of couple-stresses in linear elasticity. *Archive for Rational Mechanics and Analysis* **11**, 415–448.

Ponte Castañeda, P. (1987). Asymptotic fields in steady crack growth with linear strain-hardening. *Journal of the Mechanics and Physics of Solids* **35**, 227–268.

Radi, E. (2003). Strain-gradient effects on steady-state crack growth in linear hardening materials. *Journal of the Mechanics and Physics of Solids* **51**, 543–573.

Shi, M.X., Huang, Y., Gao, H. and Hwang, K.C. (2000). Non-existence of separable crack-tip field in mechanism-based strain gradient plasticity. *International Journal of Solids and Structures* **37**, 5995–6010.

Toupin, R.A. (1962). Elastic materials with couple-stresses. *Archive for Rational Mechanics and Analysis* **11**, 385–414.

Vardoulakis, I., Exadaktylos, G. and Aifantis, E. (1996). Gradient elasticity with surface energy: mode-III crack problem. *International Journal of Solids and Structures* **33**, 4531–4559.

Wei, Y. and Hutchinson, J.W. (1997). Steady-state crack growth and work of fracture for solids characterized by strain gradient plasticity. *Journal of the Mechanics and Physics of Solids* **45**, 1253–1273.

Xia, Z.C. and Hutchinson, J.W. (1996). Crack-tip fields in strain gradient plasticity. *Journal of the Mechanics and Physics of Solids* **44**, 1621–1648.

Yavari, A., Sarkani, S. and Moyer E.T. Jr., (2002). On fractal cracks in micropolar elastic solids. *Journal of Applied Mechanics* **69**, 45–54.

Zhang, L., Huang, Y., Chen, J.Y. and Hwang, K.C. (1998). The mode III full-field solution in elastic materials with strain gradient effects. *International Journal of Fracture* **92**, 325–348.